Department of Biomedical Sciences
University of Veterinary Medicine Vienna

Institute for Medical Biochemistry
(Head: Univ.-Prof. Dr. rer. nat. Florian Grebien)

# Validation of candidate genes controlling migration and proliferation of melanoma brain metastasis - Focus on the nerve growth factor receptor and its intracellular domain

Diploma thesis submitted for the fulfillment of the requirement for the degree of
**Magister medicinae veterinariae**

University of Veterinary Medicine Vienna

submitted by
Chloé Marie Barthelemy

Vienna, August 2022

Supervisor: Univ.-Prof. Dr. rer. nat. Florian Grebien
University of Veterinary Medicine Vienna
Department of Biomedical Sciences
Institute for Medical Biochemistry
Veterinärplatz 1
1210 Vienna

# Table of Contents

# List of abbreviations

**APS –** Ammonium persulfate

**BM** – brain metastases

**BMC1 –** brain metastasis-derived cell line 1

**BRAF –** B-rapidly accelerated fibrosarcoma

**CAS9** – CRISPR-associated protein 9

**CNS –** central nervous system

**CRISPR –** clustered regularly interspaced short palindromic repeats

**CTF –** C-terminal fragment

**CTLA-4 –** cytotoxic T-lymphocyte associated protein 4

**DMEM –** Dulbecco's modified eagle medium

**DMSO –** dimethyl sulfoxide

**DNA –** deoxyribonucleic acid

**DTIC –** dacarbazine

**DTT –** dithiothreitol

**FAP –** fibroblast activation protein alpha

**FBS –** fetal bovine serum

**FDA-** food and drug administration

**GFP –** green fluorescent protein

**GTP –** guanosine triphosphate

**HSPE1 –** heat shock protein family E, member 1

**ICD –** intracellular domain

**IL-2 –** interleukin-2

**IMP –** Research Institute of Molecular Pathology, Vienna

**iRFP –** near-infrared fluorescent protein

**kDA –** kilodalton

**LB –** lysogeny broth

**LoF** – loss of function

**MAPK –** mitogen-activated protein kinase

**MEK –** mitogen-activated protein kinase

**NaF –** sodium fluoride

**NF1 –** neurofibromin 1

**NF-κB –** nuclear factor kappa-light-chain-enhancer of activated B cells

**NGFR –** nerve growth factor receptor

**NRAS –** neuroblastoma-type ras sarcoma virus

**OS –** overall survival

**PBS –** phosphate-buffered saline

**PD-L1 –** programmed death-ligand 1

**PD-1 –** programmed cell death protein 1

**PFS –** progression-free survival

**PI –** protease inhibitor

**PI3K –** phosphoinositide 3-kinase

**PMSF –** phenylmethylsulfonyl fluoride

**PTEN –** phosphatase and tensin homolog

**P/S –** penicillin/streptomycin

**Q61L –** substation of leucine for glutamine at position 61

**RECIST –** response evaluation criteria in solid tumors

**RIPA –** Radioimmunoprecipitation assay

**RNA –** ribonucleic acid

**sgRNA –** single guide RNA

**shRNA –** short hairpin RNA

**TEMED –** tetramethylethylenediamine

**TNFα -** tumor necrosis factor-alpha

**TPCK –** 1-Tosylamide-2-phenylethyl chloromethyl ketone

**V600E –** substitution of valine for glutamic acid at position 600

**WT –** wild-type

## 1. Abstract

Melanoma is the 5th most common cancer diagnosis in the United States and is the 17th most common cancer worldwide. Early diagnosis is linked with a good prognosis; however, the overall survival drops drastically once the tumor metastasizes to distant organs such as lung, liver and brain.

For this study, we were particularly interested in the nerve growth factor receptor (NGFR), since it seems to be a key player in the development of metastases as well as in the development of acquired resistances to therapy in melanoma patients.

In order to decipher the potential mechanisms of NGFR-driven process, we aimed to establish a knockout of NGFR in a melanoma brain metastasis-derived (BMC) cell line by CRISPR/Cas9-technology and a set of 9 single guide RNAs (sgRNAs) targeting different exons of the NGFR gene. Although we observed a strong decrease in cell viability and proliferation by shRNAs targeting exon 3 of NGFR, sgRNAs were not effective. A western blot revealed the presence of a intracellular domain (ICD) fragment that might rescued knockout cells from cell death. Could the ICD fragment be responsible for restoring cell viability in the NGFR knock-out cell lines? In order to answer this question, we performed knock-outs of the ICD coding exons and used the proteasome inhibitor MG132 in order to stop the proteasomal degradation of the ICD fragment.

However, we were not able to solve the question if the ICD fragment is able to rescue the negative effects of the NGFR knock-out. In fact, more experiments would be needed to reach a final conclusion.

## 2. Zusammenfassung

Das Melanom ist die fünfthäufigste Krebsdiagnose in den Vereinigten Staaten und die 17. häufigste Krebsart weltweit. Eine frühzeitige Diagnose ist mit einer guten Prognose verbunden; allerdings sinkt die Gesamtüberlebensrate drastisch, sobald der Tumor in entfernte Organe wie Lunge, Leber und Gehirn metastasiert.

Für diese Studie interessierten wir uns besonders für den Nervenwachstumsfaktor-Rezeptor (NGFR), da er eine Schlüsselrolle bei der Entstehung von Metastasen sowie bei der Entwicklung von erworbenen Therapieresistenzen bei Melanompatienten zu spielen scheint.

Um die potenziellen Mechanismen NGFR-gesteuerter Prozesse zu entschlüsseln, haben wir versucht, NGFR in einer Melanom-Zelllinie, die aus einer Hirnmetastase abgeleitet wurde (BMC), mittels CRISPR/Cas9-Technologie und einer single guide RNAs (sgRNAs), die an verschiedene Exons des NGFR-Gens binden, auszuschalten. Obwohl wir einen starken Rückgang der Vitalität und Proliferation der Zellen durch shRNAs, die auf das Exon 3 des NGFR-Gens abzielen, beobachten konnten, waren die sgRNAs nicht wirksam. Ein Western Blot zeigte das Vorhandensein eines intrazellulären, NGFR-abgeleiteten Fragments (ICD), das Zellen mit einem Knockout möglicherweise vor dem Zelltod bewahren könnte. Könnte das ICD-Fragment für die Wiederherstellung der Fitness in den NGFR-Knockout-Zelllinien verantwortlich sein? Um diese Frage zu beantworten, haben wir Knock-outs der ICD-kodierenden Exons durchgeführt und den Proteasom-Inhibitor MG132 eingesetzt, um den proteasomalen Abbau des ICD-Fragments zu stoppen.

Wir waren jedoch nicht in der Lage, die Frage zu beantworten, ob das ICD-Fragment in der Lage ist, die negativen Auswirkungen des NGFR-Knock-outs zu beheben. Es sind daher weitere Experimente erforderlich um die Rolle des ICD-Fragments genauer zu untersuchen.

# 3. Introduction

## 3.1. Melanoma

According to the National Cancer Institute, malignant melanoma is the 5th most common cancer diagnosis in the U.S., it represents 5,6% of all new cancer cases and the incidence keeps rising.

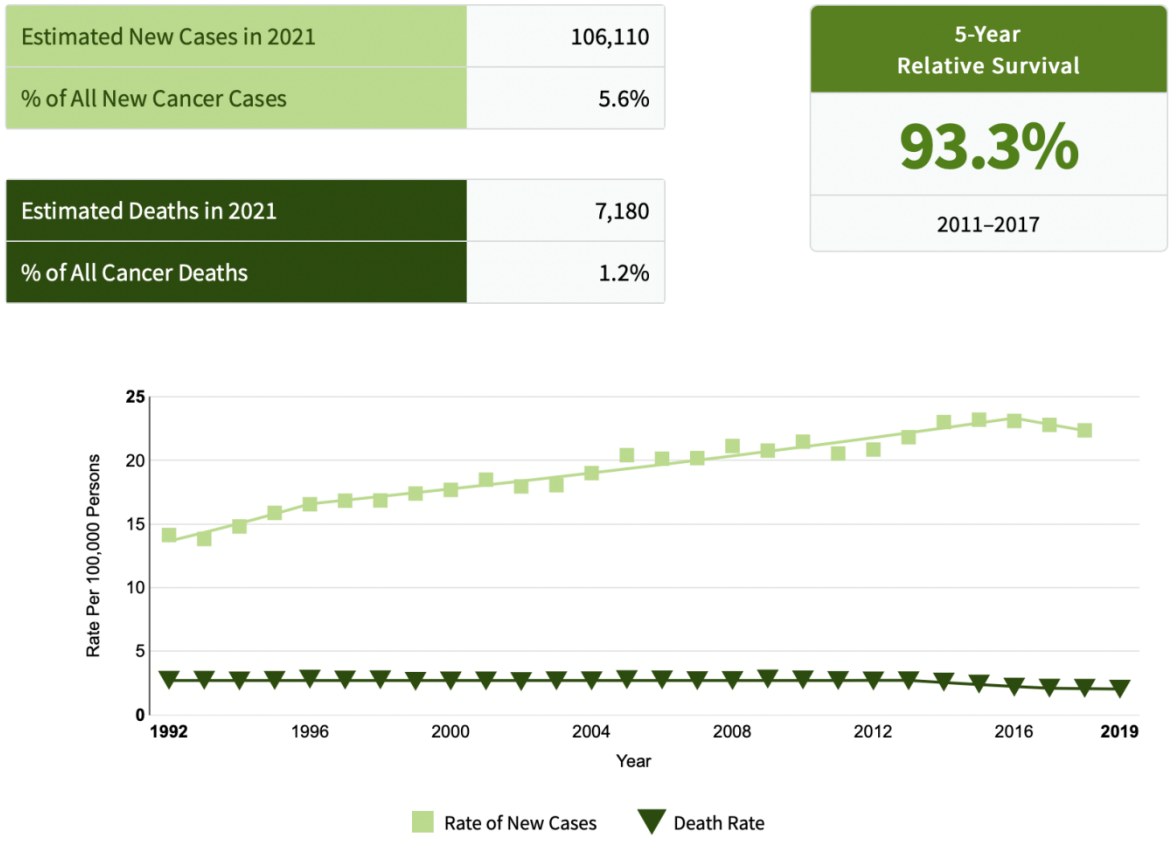


**Figure 1 - Development of melanoma cancer cases over the years**

The incidence of new melanoma cases keeps rising throughout the years. In 2021, there were an estimated 106'110 new cases of melanoma in the US and the death cases were estimated to 7180. The 5-year survival rate from 2011-2017 for stage I melanoma was 93,3%.

*Source: National Cancer Institute https://seer.cancer.gov/statfacts/html/melan.html*

Melanoma is defined by the malignant transformation of melanocytes, which arise from neural crest cells and are responsible for the production of a pigment known as melanin. Since melanocytes can be found in different parts of the body, we can histologically discriminate between different types of melanoma, such as mucosal melanoma, ocular melanoma, metastatic melanomas from unknown primary sites and presumed primary visceral melanomas (DeVita et al., 2011). However, cutaneous melanoma is the most common manifestation of this disease. According to the National Cancer Database, it is responsible for over 90% of all melanoma diagnoses in the United States.
Four main subtypes can be defined for cutaneous melanoma, including nodular melanoma, acral lentiginous melanoma, lentigo maligna and superficial spreading melanoma, with the last one being the most common one (Gray-Schopfer et al., 2007).

Based on the staging system, which considers tumor thickness, ulceration of the primary tumor, number of affected lymph nodes and presence of distant metastatic melanoma we can distinguish between 4 main stages for malignant melanoma (Kim et al., 2002).
Stage I and II are considered as early stages. There is no involvement of the lymph nodes yet. We differentiate between stage I and II based on tumor thickness and ulceration.
Stage III melanoma shows involvement of the lymph nodes. Stage IV is defined by the presence of distant metastases (Balch et al., 2009).

The 5-year relative survival for stage I melanoma is > 90% when diagnosed early. However, the overall survival (OS) drops drastically to a 10-year survival rate < 10% (Bhatia et al., 2009), for stage IV melanoma.

### 3.2. Genomic classification of melanoma

The presence of oncogenic mutations, hence mutations that either lead to the constitutive activation of signaling pathways, such as mutations in B-rapidly accelerated fibrosarcoma (BRAF) or neuroblastoma-type ras sarcoma virus (NRAS), as well as loss-of-function (LOF) mutations in neurofibromin 1 (NF1), a negative regulator of RAS signaling, are the most common mutations found in melanoma. We, therefore, differentiate between four main types of melanoma, these being mutant BRAF, mutant NRAS, mutant NF1 and Triple Wild-Type (WT), which are mutated melanoma lacking BRAF, NRAS or NF1 mutations (Akbani et al., 2015).

The largest group is defined by BRAF hot-spot mutations (Akbani et al., 2015), which are found in 50-70% of all cutaneous melanoma. The most common mutation in this group is the substitution of valine for glutamic acid at position 600 in the BRAF protein (V600E) (Gray-Schopfer et al., 2007). However, a study by Dankort et al. (Dankort et al., 2009) showed that $BRAF^{V600E}$ only leads to melanoma formation, when co-occurring with loss of the Phosphatase and Tensin homolog (PTEN), which is a negative regulator of the Phosphoinositide 3-kinase (PI3K)-pathway. This indicates that the presence of $BRAF^{V600E}$ as well as the activation of PI3K, might need to occur together for brain metastasis to form (Redmer, 2018).

BRAF is directly involved in the Mitogen-activated Protein Kinase (MAPK) pathway (Y. Guo et al., 2020). The mutation of BRAF results in a higher activity of the mitogen-activated protein kinase, which leads to the loss of dependency on upstream signaling events. The MAPK pathway is responsible not only for cellular proliferation but also for gene expression, cell differentiation, mitosis, cell survival and apoptosis. (Menzies et al., 2012).

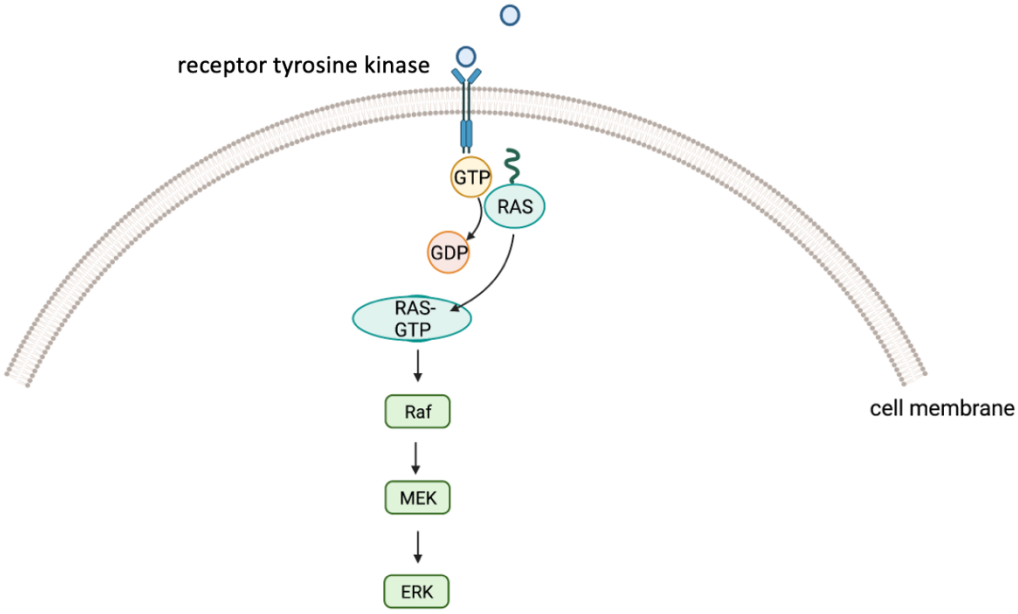


**Figure 2 - Simplified scheme of the MAPK pathway**

The MAPK pathway is activated when a ligand such as FGF2 binds to the corresponding receptor tyrosine kinase such as FGFR1. The activation of the receptor leads to the removal of a guanine diphosphate molecule from the Ras protein, which allows the binding of guanine triphosphate, leading to the activation of the Ras protein. Activated Ras is now able to activate the Raf kinase, which in turn activates MEK that in turn activates ERK by phosphorylation (McCain, 2013).

*Figure created with BioRender.com*

The second major subtype found in cutaneous melanoma is defined by RAS hot-spot mutations (Akbani et al., 2015). Mutations which lead to functional changes can be found in NRAS, as well as KRAS and HRAS. However, the most common change is a gain of function mutation (substitution of glutamine for leucine at position 61 (Q61L)) in NRAS, which accounts for 15-30% of all melanoma cases (Gray-Schopfer et al., 2007). Patients suffering from NRAS-mutated melanomas have a lower overall survival compared to BRAF mutated melanomas.

This is mostly linked to the higher aggressiveness of this kind of tumor but also due to the lack of efficient targeted therapies and the rapid development of resistance to the few available therapy options (Randic et al., 2021).

The third most frequent mutation is found in NF1. This type of mutation is mostly found in patients which are significantly older (Akbani et al., 2015). About half of the mutations in NF1 lead to the inactivation of the protein. This loss of function leads to the activation of Ras by reducing the levels of guanosine triphosphate (GTP) hydrolysis, which results in the hyper-activation of the MAPK pathway (W. Guo et al., 2021).

Lastly, we know Triple WT melanoma, which is defined by the lack of hot-spot mutations in BRAF, RAS and NF1. Triple WT melanoma seems to show an enrichment of KIT mutations as well as focal amplifications and complex structural rearrangements (Akbani et al., 2015).

### 3.3. Brain metastatic melanoma

Melanoma is considered the deadliest form of skin cancer due to its high metastatic rate. Usually, it first metastasizes to the lymph nodes before invading other organs of the body. Notably, melanoma is the cancer with the highest propensity to metastasize to the brain. After breast and lung cancer, it is the third-most frequent cause of brain metastases (Glitza et al., 2016). 10 – 40% of patients suffering from melanoma develop brain metastases (BM) at some point, however, metastatic lesions in the brain are found in 73 – 90% of melanoma patients *post-mortem*. This indicates that a high number of tumor cells are capable of infiltrating the brain, however, only a small subset of these cells form macrometastases. (Redmer, 2018).
In addition, the therapy of metastatic melanoma does not often lead to long-lasting effects. In fact, the incidence of developing resistance to therapies is very high. The combination of these factors leads to the poor prognosis. In fact, brain metastatic melanoma has a median survival rate of 6 months and a 5-year survival rate of less than 5% (Gray-Schopfer et al., 2007).

For brain metastasis to form, tumor cells have to cross the blood-brain barrier, which consists of tightly connected endothelial cells lining the cerebral microvessels as well as tight junction

proteins, such as occludins, claudins and junctional adhesion molecules, in order to successfully restrict passive diffusion. In addition, astrocytes play an important role in forming even tighter tight junctions, by lining the walls of the microvessels with their perivascular endfeet (Daneman & Prat, 2015).

To pass through the blood-brain barrier and induce the development of brain metastases, melanoma cells have to adhere to and disturb the interaction of the brain endothelial cells (Redmer, 2018). After transmigration, micrometastases can grow along the brain microvessels and lead to the formation of macrometastases (Kienast et al., 2010).

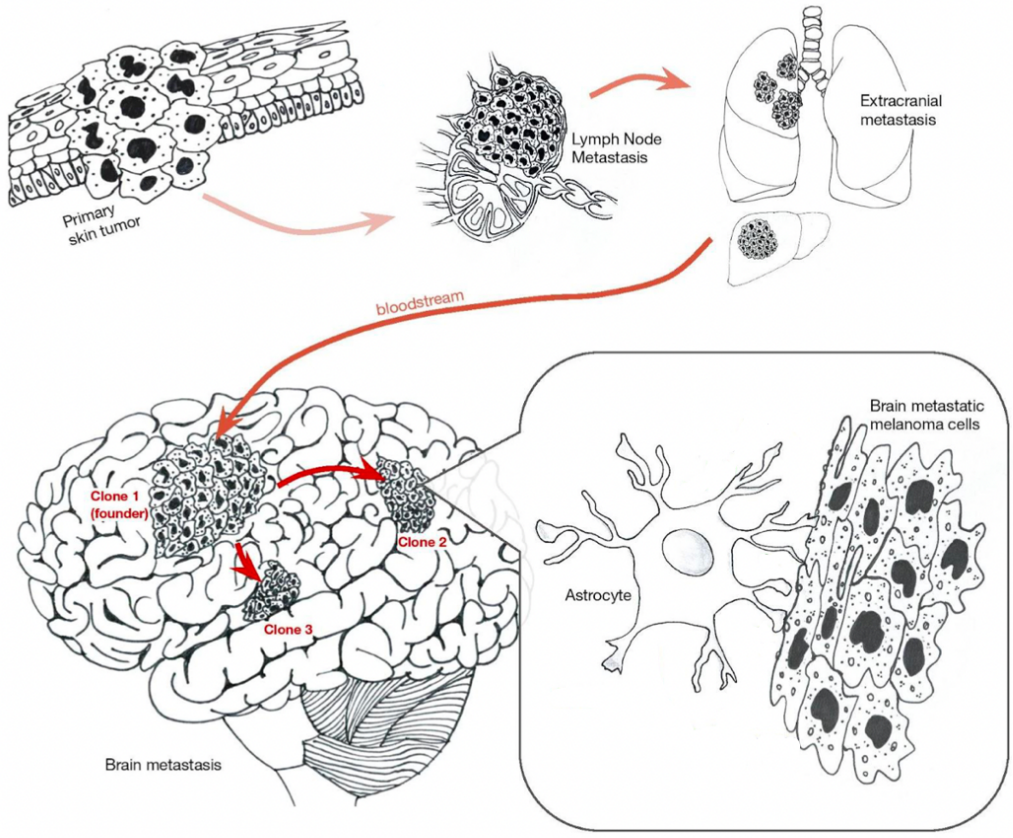


**Figure 3 - Schematic representation of melanoma brain metastasis formation**

Melanoma cells first metastasize to the lymph nodes, before metastasizing to other organs, forming not only extracranial metastases but also brain metastases. In the brain, melanoma brain metastasis cells interact closely with the astrocytes thanks to different factors.

*Source: Drawing created by Anna Vidal*

### 3.4. Therapy options for metastatic melanoma

Metastatic melanoma is very hard to treat, since it seems to be barely responsive to therapy (Gray-Schopfer et al., 2007) and rapidly acquires resistances to targeted therapies. During the last decade, a lot of work has been put into understanding the pathogenesis of melanoma to develop new therapy options with the hope to improve patient prognosis. However, one big hurdle that we still face to this day is the rapid development of therapy resistance, which leads to progressive disease (W. Guo et al., 2021).

Nowadays, the gold standard for the treatment of brain metastatic melanoma is systemic therapy using a combination of BRAF inhibitors (dabrafenib, vemurafenib) and a mitogen-activated protein kinase (MEK) 1/2 inhibitor (trametinib). In fact, this combination leads to a drastic improvement in overall survival (Redmer, 2018). Since over 50% of all metastatic melanoma are BRAF mutated, BRAF inhibitors can lead to an improvement in most patients (Curtin et al., 2005).

Vemurafenib was the first selective BRAF inhibitor to be used in clinical trials. It showed a high activity towards $BRAF^{V600E}$-mutated melanoma, compared to BRAF wildtype cases. The response evaluation criteria in solid tumors (RECIST) response rate increased to 53%, the median progression-free survival (PFS) to 6,9 months and the overall survival to 13,6 months. Dacarbazine, the drug of choice before 2010, had a RECIST response rate of 8%, a PFS of 1,6 months and a median OS of 10 months (McArthur et al., 2014).

Dabrafenib is a selective BRAF inhibitor, just like vemurafenib, and inhibits $BRAF^{V600E}$ and $BRAF^{V600K}$ mutations in metastatic melanoma. Dabrafenib has a high response rate (Objective response rate of 50% (W. Guo et al., 2021)), a quick mode of action as well as little toxicity. (Menzies et al., 2012). It should be noted that the use of BRAF inhibitors leads to the development of keratoacanthoma and squamous cell carcinoma in about 20% of all patients (W. Guo et al., 2021).

MEK inhibitors, such as trametinib, act downstream of BRAF in the MAPK signaling pathway. Although they did not show much of an effect when used in patients with unknown BRAF status, they proved effective in BRAF mutated melanoma patients, leading to impressive results (Menzies et al., 2012). In fact, according to the phase 3 open-label trial conducted by Flaherty et al. in 2012, the use of MEK inhibitors in patients suffering from BRAF mutated melanoma led to an overall response rate of 22% and a median PFS of 4,8 months (Flaherty et al., 2012). The use of MEK inhibitors alone has also been approved for non-BRAF mutated melanoma, however, the treatment outcome has not been satisfactory (W. Guo et al., 2021).

The hope of the combination treatment consisting of BRAF and MEK inhibitors is that the joint blockade of the MAPK pathway at two different levels could delay the development of acquired resistances. (Menzies et al., 2012).
Additionally, the combination of both substances leads to much higher response rates as well as longer-lasting clinical benefits, when compared to monotherapy (Menzies et al., 2012). The combined use of BRAF and MEK inhibitors not only led to an improvement in the 12-month OS (72% compared to 65% when undergoing vemurafenib monotherapy), but also significantly reduced the occurrence of keratoacanthoma and squamous cell carcinoma (1% compared to 18% when undergoing vemurafenib monotherapy)(Robert et al., 2015).

### 3.5. Resistance to therapy

Although dabrafenib is the go-to therapeutic agent, being highly effective and offering high response rates as well as a higher survival, a big problem that remains is the development of resistances to this treatment within 6-12 months (Lin & Fisher, 2017).

We differentiate between three types of resistances: intrinsic, adaptive, and acquired resistance. About 20% of BRAF-mutated melanomas do not respond to treatment with MAPK inhibitors, thus they are intrinsically resistant. This can be affiliated with multiple genomic, but also non-genomic alterations (W. Guo et al., 2021).

Adaptive resistance develops during the early phases of treatment. In order to ensure tumor cell survival, intracellular pathways are activated to protect the cell. The development of adaptive resistance does not only affect the efficacity of therapy but can also lead to the development of acquired resistances (Smith et al., 2016).

Acquired resistances arise after long-term treatment with MAPK inhibitors. They are the results of mutations, which lead to the establishment of resistant clones of tumor cells (W. Guo et al., 2021). In fact, many melanoma patients undergoing treatment show disease progression after a rapid but incomplete response to dabrafenib (Menzies et al., 2012). A study by Long et al. from 2014 showed that most melanomas resistant to treatment with BRAF inhibitors contained additional oncogenic mutations which caused reactivation of the MAPK and P13K pathways. This could be the reason why this kind of melanoma is refractory to treatment with MAPK inhibitors (Long et al., 2014).

Another theory is that the nerve growth factor receptor (NGFR) might be an important player in the development of acquired resistance. In fact, it has been proven, that NGFR levels are drastically increased in resistant cells after treatment with BRAF inhibitors (Saltari et al., 2021). The inhibitors seem to stimulate the secretion of tumor necrosis factor-alpha (TNFα), which leads to the activation of the nuclear factor kappa-light-chain-enhancer of activated B cells (NF-κB) pathway, resulting in a higher expression of NGFR. The inhibition of the TNFα/NF-κB pathway in combination with the silencing of NGFR led to restored sensitivity to BRAF inhibitors (Lehraiki et al., 2015).

Additionally, a study by Filipp et al. from 2019 found that increased levels of NGFR led to increased resistance to chemotherapeutic agents as well as evasion from the immune system through de-differentiation and downregulation of antigen that activate T-cells (Filipp et al., 2019). Also, the combined use of antibodies targeting CD46 and NGFR prevented the development of melanoma metastases in vivo (Ngo et al., 2016).

These data make NGFR an interesting potential therapeutic target in melanoma. We must keep in mind though, that NGFR is not only present on melanoma cells. Targeting NGFR in melanoma patients could affect the functions of astrocytes and neurons.

### 3.6. Nerve growth factor receptor (NGFR)

The nerve growth factor receptor (NGFR, also known as CD271 or $p75^{NTR}$) is a transmembrane protein which belongs to the TNF receptor family. It is responsible for a multitude of functions in the central nervous system (CNS), including the regulation of neuronal survival, apoptosis, myelination and axonal regeneration. It responds to the binding of different ligands such as NGFR, NT, BDNF, NT3, NT4/5 as well as their respective pro-neurotrophins (Chen et al., 2009)(Vidal & Redmer, 2020). Upon binding, NGFR may form different cleavage products, such as the intracellular domain (ICD) or the C-terminal fragment (CTF).

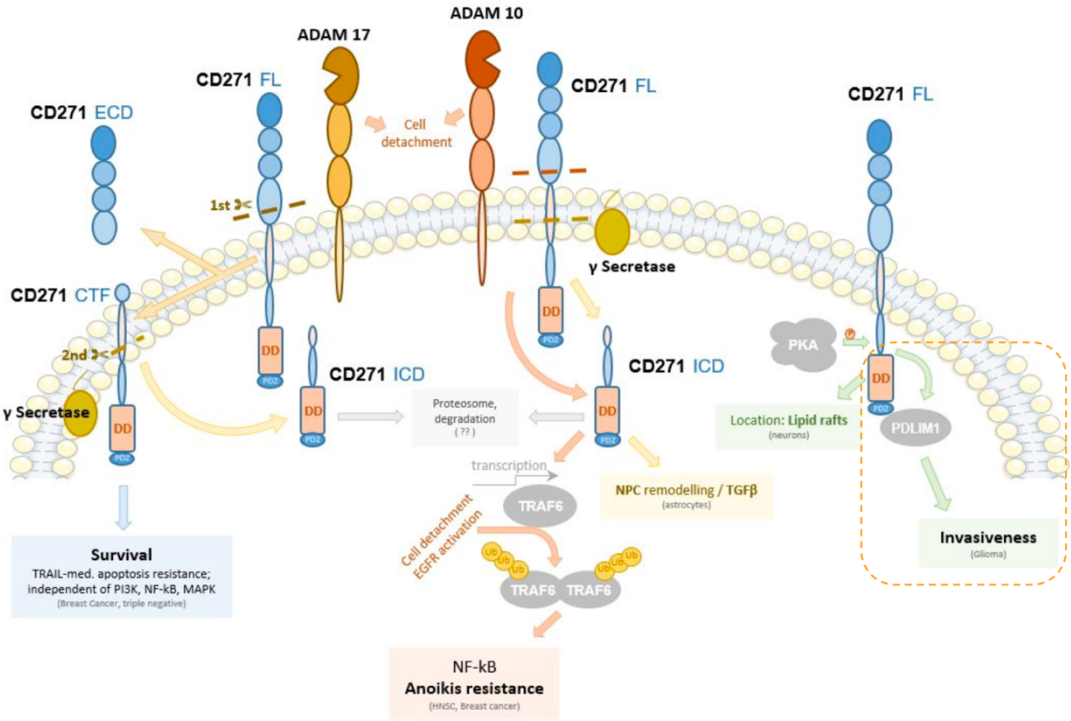


**Figure 4 - The NGFR signaling pathway**

This drawing shows NGFR signaling pathway connected to NGFR cleavage. The full-length NGFR can be clipped, which results in either the intracellular domain or the C-terminal fragment. The C-terminal fragment is responsible for survival. The intracellular domain undergoes proteasomal degradation in the cell and can lead to anoikis resistance.

*Source: Figure taken from Vidal & Redmer, 2020*

Melanocytes are derived from neural crest cells during embryonic development and retain the expression of NGFR. NGFR is considered a very potent cancer stem cell marker in melanoma, allowing their identification and isolation (Boiko et al., 2010). However, the different functions of NGFR are still not fully understood, even though the molecule has been known for over 50 years and its important role in melanoma has been studied for the last 4 decades already.

In normal melanocytes, among other functions, NGFR is responsible for skin differentiation processes. However, in melanoma, NGFR promotes tumor progression. In fact, Filipp et al. demonstrated in 2019 that NGFR expression can lead to the activation or repression of different genes responsible for differentiation and cell death in physiological tissues, which leads to self-renewal and survival in melanoma. As such, NGFR can be considered a molecular switch controlling the proliferation and the stem-like migration phenotype in melanoma tumor cells (Filipp et al., 2019).

Already in 1993, Herrmann et al. were able to establish a link between a highly aggressive tumor with a high metastatic rate and elevated levels of NGFR (Herrmann et al., 1993). In 2008, Truzzi et al. demonstrated that NT-3, NT-4 and NGF led to a more extensive migration of metastatic melanoma cells. They also established a direct link to NGFR. In fact, when NGFR was knocked down, no proNGF cell migration could be observed (Truzzi et al., 2008).
Additionally, in 2014, Redmer et al. demonstrated that the knockdown of NGFR in a patient-derived melanoma cell line led to a strong decrease in tumor-forming capacity (Redmer et al., 2014). These studies show the correlation between NGFR and aggressive disease progression, including a higher metastatic rate.

NGFR expression in cultured cells is very unstable and depends on many factors. Cellular stress, induced by therapy, for example, can lead to increased levels of NGFR, which in turn leads to the development of resistance (Menon et al., 2015), as discussed in the last chapter. A study by Restivo et al. suggests that low levels of NGFR promote proliferation, whereas high levels of NGFR lead to invasiveness, hence the level of NGFR expression determines proliferative and migratory phenotypes in melanoma and might suggest the presence of an intermediate cell state capable of proliferation and migration. According to this theory, initial

tumor growth would be defined by low NGFR levels, allowing the cells to proliferate. The cells would then metastasize at higher NGFR levels and finally grow again at lower NGFR levels once they have reached their distant metastatic site (Restivo et al., 2017).

For my project, we were particularly interested in the intracellular domain (ICD) of NGFR, which is functionally not well characterized.
The ICD fragment is defined as a cleavage product of NGFR and contains the death domain and likely controls cell proliferation (Restivo et al., 2017), but might also be involved in other cell processes, such as apoptosis. In fact, Saltari et al. showed that the cleavage of the ICD fragment by a beta-amyloid-derived peptide led to apoptosis as well as reduced metastasis *in vivo*. They also stated that mutations in the ICD might prevent cell death (Saltari et al., 2021).
However, a study by Bao et al. from 2018 has shown that ADAM10-mediated NGFR cleavage results in the formation of ICD fragments. These fragments protect the cells from anoikis, a special kind of programmed cell death linked to the detachment of cells from the extracellular matrix, by activation of the NFκB pathway (Bao et al., 2018).

### 3.7. CRISPR-Cas9

The Clustered Regularly Interspaced Short Palindromic Repeats-Cas CRISPR-associated protein 9 (CRISPR-Cas9) is an important genome editing tool, allowing specific genes to be knocked out (Doudna & Charpentier, 2014). The CRISPR-Cas9 system originates in prokaryotic organisms, where it is part of the adaptive immunity (Barman et al., 2020).
The CRISPR-Cas9 system includes the Cas9 nuclease and a guide RNA (gRNA). The 20 bp gRNA mediates the recognition of a specific DNA target. After binding, the gRNA recruits the Cas9 nuclease, which in turn generates double-stranded breaks in the DNA. Cells try to repair the damage caused by the CRISPR-Cas9 system by activating their error-prone non-homologous end joining repair pathway, which in turn leads to insertion/deletion mutations, resulting in the knockout of the targeted gene (Sun et al., 2016).

For our experiments, we used the CRISPR-Cas9 system in melanoma cell lines to knock-out a certain gene and study its effects.

### 3.8. Preliminary work

In previous experiments conducted by Anna Vidal and Torben Redmer, they observed a difference in the growth of melanoma cells when comparing the knock-out, using the CRISPR-Cas9 system and the knock-down, using inducible short hairpin ribonucleic acid (shRNA) targeting NGFR, as shown in the following graphs:

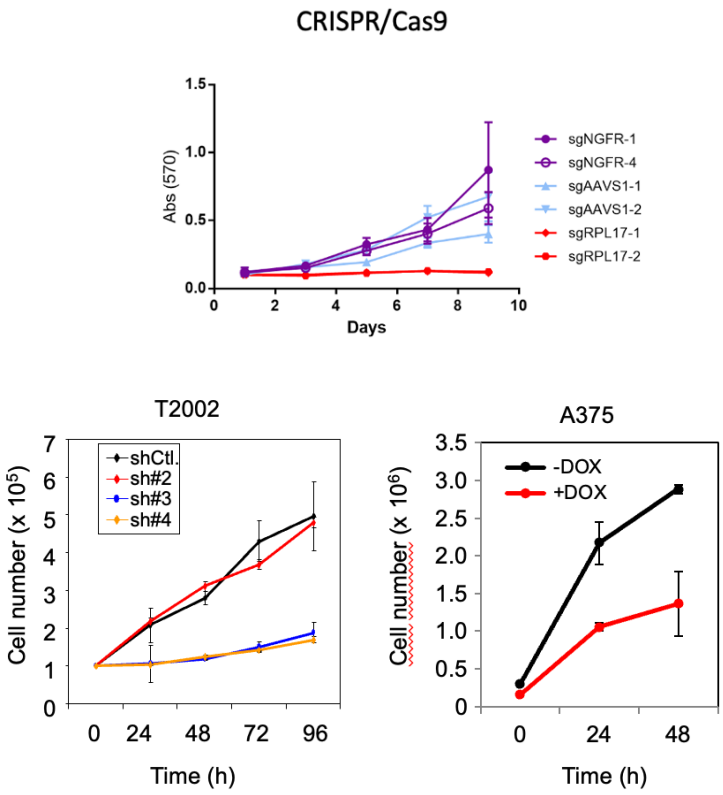


**Figure 5 - Comparison of NGFR Knock-out vs. Knock-down**

When NGFR was knocked out using the CRISPR Cas-9 system in the BMC1 cell line, we were not able to observe a reduction in cell growth when comparing the knock-out cell line to the negative control (sgAAVS1). However, when inducing a NGFR knock-down using inducible shRNA, as in the A375 cells, or with a constitutively expressed shRNA as in the T2002 cells, a clear downregulation of cell growth was observed compared to the controls.

After observing the difference in cell growth, when comparing NGFR knock-out and knock-down, we performed a Western blot to make sure, that the Knock-out worked properly and led to a complete loss of protein expression.

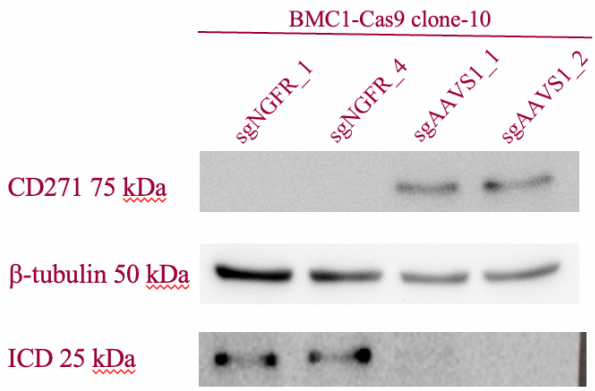


**Figure 6 - Western blot of BMC1-Cas9 clone 10 knock-out for CD271 (NGFR)**

Western blot of CRISPR-edited BMC1-Cas9-clone 10 comparing the use of sgNGFR_1 and sgNGFR_4, using sgAAVS1_1 and sgAAVS1_2 as positive controls for CD271 (NGFR) expression. A polyclonal antibody targeting CD271 as well as a monoclonal antibody targeting β-tubulin as a loading control were used.

Although we could not observe the expression of the full length-fragment of NGFR, expected at 75 kilodalton (kDa), in the NGFR knock-out cell lines using sgNGFR_1 and sgNGFR_4, we could appreciate a light band that appeared at 25 kDa. After doing some research on NGFR, we concluded that this band could represent the expression of the intracellular domain (ICD). Thus, we hypothesized that the ICD fragment could be responsible for rescuing the expected effect of the NGFR knock-out. Investigation of the NGFR gene sequence identified an in-frame ATG codon at position 236, which was surrounded by a Kozak sequence, which is required for efficient initiation of translation. The predicted molecular weight of this new fragment is 22 kDa, which would also correlate with the size of the fragment we observed in the previous Western blot. It is important to note that sgNGFR_1, as well as sgNGFR_4 both target the NGFR N-terminus upstream of the new translation initiation site at position 236 (Figure 7). This led us to the conclusion that even if the knock-out using these guides works properly, the ICD fragment can still be produced.

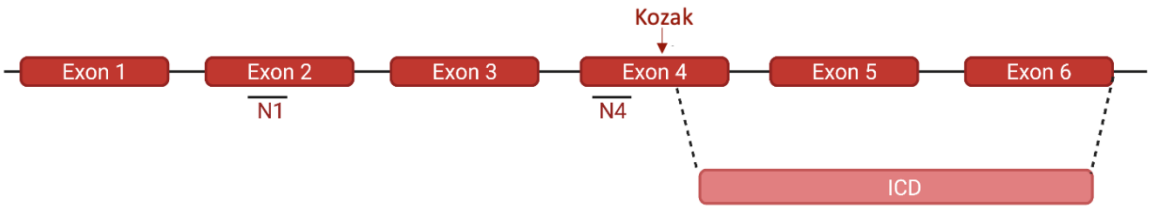


**Figure 7 - Position of sgNGFR_1 & 4**

sgNGFR_1 targets Exon 2 and sgNGFR_4 targets Exon 4. The in-frame ATG codon surrounded by the Kozak sequence is also located in Exon 4. However, it is located after the sequence targeted by sgNGFR_4

### 3.9. Aim of the study/Hypothesis

Following the results of the previous investigations, we asked whether expression of the predicted 22kDa ICD fragment could be responsible for restoring cell viability in the NGFR knock-out cell lines. To answer this question, we aimed to achieve a complete and reproducible knock-out of NGFR using different single guide RNAs (sgRNAs) and sgRNA combinations. In addition, we aimed to conduct further experiments to characterize the role of the presumed NGFR ICD fragment itself.

# 4. Material and Methods

## 4.1. Cell lines

To conduct our experiments, we used a stable cell line that was established from a brain metastasis of a melanoma patient in 2018 (brain metastasis derived cell line 1 (BMC1)). This cell line serves as a suitable in vitro system for modeling drug responses and cellular dependencies. In order to investigate the role of NGFR by CRISPR/Cas9-mediated genome engineering, we established a Cas9-expressing system. The Cas9-expressing cell line was produced by PhD Student Anna Vidal in the lab by lentiviral transduction of cells with a plasmid carrying the coding sequence of Cas9. In addition, Cas9 expression was coupled to the expression of green fluorescent protein (GFP), enabling the isolation of GFP-positive cell clones. Following infection, cells were sorted for green fluorescent protein (GFP) expression using the single-cell sorting method to generate clonal populations from single cells.
To effectively use the Cas9 system and be able to extract functional conclusions of the gene that is being targeted, it is important to choose clones, which show a homogenous and stable expression of Cas9. This led to our decision to use the BMC1-Cas9 clone 8 and 10.

We also used the cell line A375, which is a common and commercially available non-metastatic melanoma cell line for a different experiment.

All cell lines were cultured in Dulbecco's modified eagle medium (DMEM) with Penicillin/Streptomycin (P/S) (1%) and fetal bovine serum (FBS) (10%)

### 4.2. CRISPR Cas9 single guide RNA (sgRNA)

Our goal was to achieve a complete knock-out of NGFR, using the CRISPR Cas-9 system. In order to do so, we designed different sgRNAs targeting different exons of NGFR. We also used different combinations of the sgRNAs. A total of 9 sgRNAs targeting NGFR as well as control sgRNAs targeting sgRPL17 and sgAAVS1 as positive and negative controls were used.

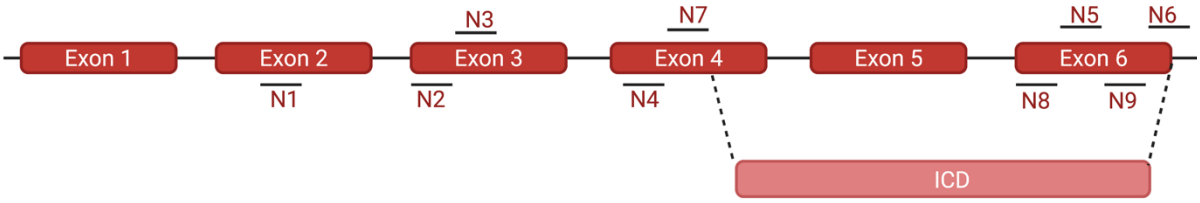


**Figure 8 - Position of the sgRNAs targeting NGFR**

We used 9 different sgRNAs targeting NGFR to induce a knock-out of NGFR. sgNGFR_1 is located in Exon 2. sgNGFR_2 & 3 are located in Exon 3. sgNGFR_4 & 7 are located in Exon 4. And sgNGFR_5, 6, 8 & 9 are located in Exon 6. The in-frame translation site is located in Exon 4.
*Figure made with BioRender.com*

### 4.3. Target guide sequence cloning and mini prep

#### 4.3.1. Backbone digestion

To incorporate the sgRNA into the lentiviral expression backbone plasmid, the backbone plasmid was digested using the restriction enzyme BsmBI. BsmBI recognizes and cuts at CGTCTC(1/5)^ sites in our vector backbone (pLenti hu6-sgRNA-IT-PGK-iRFP670). To purify the linearized vector backbone, the BsmBI digested plasmid underwent gel extraction using the MiniPEx 3 in 1 kit from the Research Institute of Molecular Pathology (IMP), Vienna.

### 4.3.2. Annealing

We then performed phosphorylation and annealing of sgRNA oligonucleotides by mixing 100 μM of each oligonucleotide and adding 10X T4 ligation buffer as well as T4 polynucleotide kinase. To initiate the phosphorylation reaction, the mix was incubated in a thermocycler at 37°C for 35 min followed by 95°C for 5 minutes and then ramped down to 25°C at 5°C/min. The annealed oligonucleotides were then diluted 1:200 into sterile water.

### 4.3.3. Ligation

To set up the ligation reaction, 50 ng of purified plasmid were mixed with the diluted oligonucleotides as well as T4 ligase and incubated at room temperature for 10 minutes. A negative control (vector backbone only) was also set up.

### 4.3.4. Transformation into competent bacteria

Following the ligation reaction, we transformed the plasmids into Stbl3 bacteria. We mixed 15μl of Stbl3 bacteria with 1-2 μl of ligated DNA and incubated the mix on ice for 10 minutes. The bacteria then underwent a heat shock at 42°C for 45 seconds and were put on ice for another 2 minutes. We then added lysogeny broth (LB) media and incubated the mix in a shaker at 37°C for 30 minutes.
The bacteria were plated on LB media with Carbenicillin (as the vector backbone contains a Carbenicillin resistance gene) and incubated overnight at 37°C.

Selected colonies, which resulted from the overnight growth of transformed bacteria, were inoculated into liquid LB media and incubated at 37°C overnight. The negative control, containing only the digested backbone without any insert should not have given rise to any colonies.

#### 4.3.5. Plasmid DNA extraction

Plasmid DNA isolation was performed using the Mini prep kit from IMP. We pelleted the overnight bacterial culture by centrifugation and removed the supernatant. We then resuspended the pelleted bacterial cells in 250µl of resuspension buffer and transferred the suspension into an Eppendorf tube. We added 250 µl of lysis buffer and 350µl of neutralizing buffer, mixing thoroughly after each step. The mixture was centrifuged for 10 minutes at 13000 rcf and the supernatant was transferred into the spin column. The spin column was centrifuged and the supernatant was discarded. We repeated this step while adding 0,75 ml of wash buffer. The DNA was then eluted using 30 µl of elution buffer and centrifuging the spin column. We then proceeded to measure the DNA concentration of our samples using the TECAN Spark, which measures UV-light absorbance at 230, 260 and 280 nm.

#### 4.3.6. Transfection

The lentivirus production and BMC1 cell transfection work were performed by PhD Student Anna Vidal.

### 4.4. Competition assay

In order to run a competition assay, we mixed 50% of cells containing the Cas9 construct but no sgRNA with 50% of sgRNA-expressing cells (infection rate: 90-100%). The cells were grown on 24 well plates. To measure the cells, we removed the media and performed 2 washes with phosphate-buffered saline (PBS). We trypsinized the cells before adding some fresh DMEM, which contains P/S as well as FBS. The FBS is needed to stop the trypsinization reaction.

The cells were thoroughly resuspended in the fresh media before a part of the mix was added to a 96-well plate. The wells were then read using the IQue Screener. In the setup used by us, Cas9 expression is coupled to GFP, while the sgRNA-expression construct carries an iRFP670 selection marker.

We are interested in the percentage of near-infrared fluorescent protein (iRFP) positive cells from the GFP-positive cells, since these are the cells that integrated the backbone plasmid as well as our sgRNA. In fact, sgRNAs, which induce deleterious mutations, will lead to a proliferative disadvantage, shown by the reduction of the iRFP signal. However, if a sgRNA induces a fitness-increasing mutation, this will lead to an increase of the iRFP signal over time.

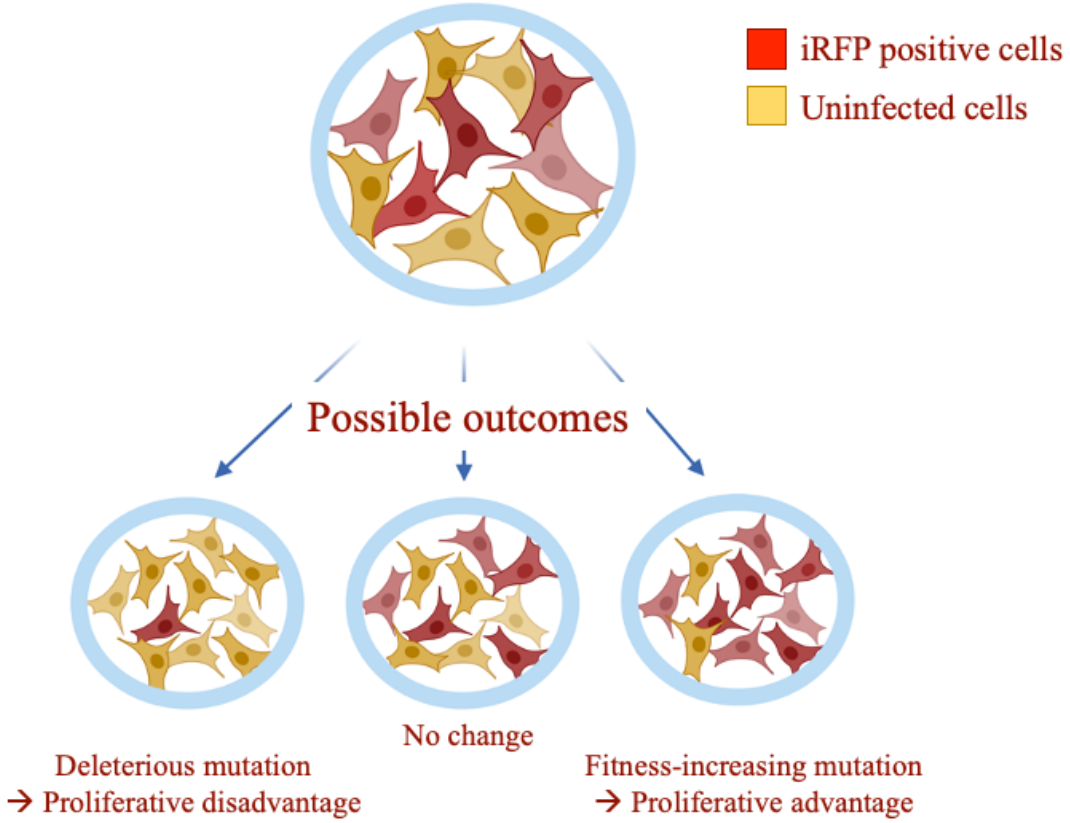


**Figure 9 - Simplified scheme of a competition assay**

For the competition assay, we mixed 50% of cells infected with a construct that carried an NGFR-targeting sgRNA and the coding sequence for iRFP670 (red) with 50% of uninfected cells (yellow). We measure the cell count of iRFP670-positive cells from the GFP-positive cells at different time points, in order to assess the survival and proliferation of our infected cells.

*Figure made with BioRender.com*

### 4.5. Western Blot

Cell pellets were lysed using a Radioimmunoprecipitation assay (RIPA) Buffer (10mM TRIS pH 8.0, 1mM EDTA, 1% NP40, 0.1% SDS, 140 mM NaCl, 0,1% Na Deoxycholate) supplemented with a Protease inhibitor (PI) cocktail (4%), Sodium fluoride (NaF) (500mM), phenylmethylsulfonyl fluoride (PMSF) (100 mM), dithiothreitol (DTT) (1M), Benzonase (25 U/µl), 1-Tosylamide-2-phenylethyl chloromethyl ketone (TPCK) (5 mg/mL). To assess the protein concentration, we performed a Bradford assay using standards with bovine serum albumin. The absorbance was read at 595nm.

We prepared the running gel using a gel buffer (1.5 M Tris-HCL pH 8.8, 0.4% SDS) Acrylamide (30%), distilled water, Ammonium persulfate (APS) (10%) and tetramethylethylenediamine (TEMED). We chose the Acrylamide concentration according to the following table:

| % Acrylamide | Molecular Mass Range |
|---|---|
| 7 | 50 kDa – 500 kDa |
| 10 | 20 kDa – 300 kDa |
| 12 | 10 kDa – 200 kDa |
| 15 | 3 kDa – 100 kDa |

**Table 1 - Acrylamide concentration for Western blot gel**

For the stacking gel, we used a gel buffer (0.5M Tris HCl, pH 6.8, 0.4% SDS), distilled Water, Acrylamide (30%), APS (10%), TEMED.

Protein lysates were mixed with Lämmli-Buffer (4x) (0.250M Tris-HCl pH 6.8, 40% Glycerol, 8% SDS, distilled water, bromophenol blue). Before use, we added β-mercaptoethanol (10%) to the Lämmli-Buffer. The gel was run through a chamber using a running buffer (SDS running buffer 10x (250mM Tris, 1.9M Glycin, 35mM SDS), distilled water). To start, we ran the gel at 80V, until the samples passed through the separation gel and then increased the voltage to 130V after that.

To transfer the gel to a membrane, the gel was placed onto a well-soaked PTFE-membrane-filter paper stack. To soak, we used 10% transfer buffer (1x) (transfer buffer 10x (Tris[hydroxymethyl]aminomethane [30,2g/L], glycine [144 g/L], water), 10% methanol, distilled water). The gel was then transferred to a membrane using a Trans-Blot Turbo Transfer Device from BioRad, we ran the turbo blot twice. The membranes were blocked using 5% low-fat milk, produced by diluting dried milk in TBS/T for one hour. To produce the TBS/T buffer, we used 10% TBS 10x pH 7.4 (1.5M NaCl, 0.5M Tris-HCl), 0.1% Tween20 and distilled water.

After the blocking, the membrane was incubated with the primary antibody overnight. Then, the membrane was incubated with the secondary antibody for 1 hour at room temperature. We developed the images with VILBER using a mix of Luminol enhancer and peroxide and repeated this with the loading control.
In between every antibody and before developing, the membrane was washed 2 times with TBS-T for 5 minutes.

We used a polyclonal antibody from Cell Signaling technology targeting NGFR (#8238) as a primary antibody and an antibody targeting β-tubulin (#2146) as a loading control.
As a secondary antibody, we used an anti-mouse antibody linked with HRP (cell signaling #7076) for β-tubulin and an anti-rabbit antibody linked with HRP (cell signaling #7074) for NGFR. The secondary antibody must be linked with HRP in order to be able to visualize them using chemiluminescence.

### 4.6. Proteasome inhibitor MG132

In order to investigate whether the ICD fragment is constantly generated in melanoma cells but controlled by proteasomal degradation, we hypothesized that blocking of the proteasome degradation machinery by the potent proteasome inhibitor MG132 might stabilize the fragment. Stabilized ICD then would be accumulated and can be detected by western blotting. According to previous experiments performed in the laboratory, we chose to treat A375 cells with the proteasome inhibitor MG132 for 8, 16 and 24 hours, using different concentrations (0,25μM, 0,5μM, 1μM, 2μM and 5μM). As a negative control, we treated the cells with DMSO.

# 5. Results

## 5.1. Growth competition assay upon CRISPR-Cas9 targeting of NGFR in BMC1 clone 10

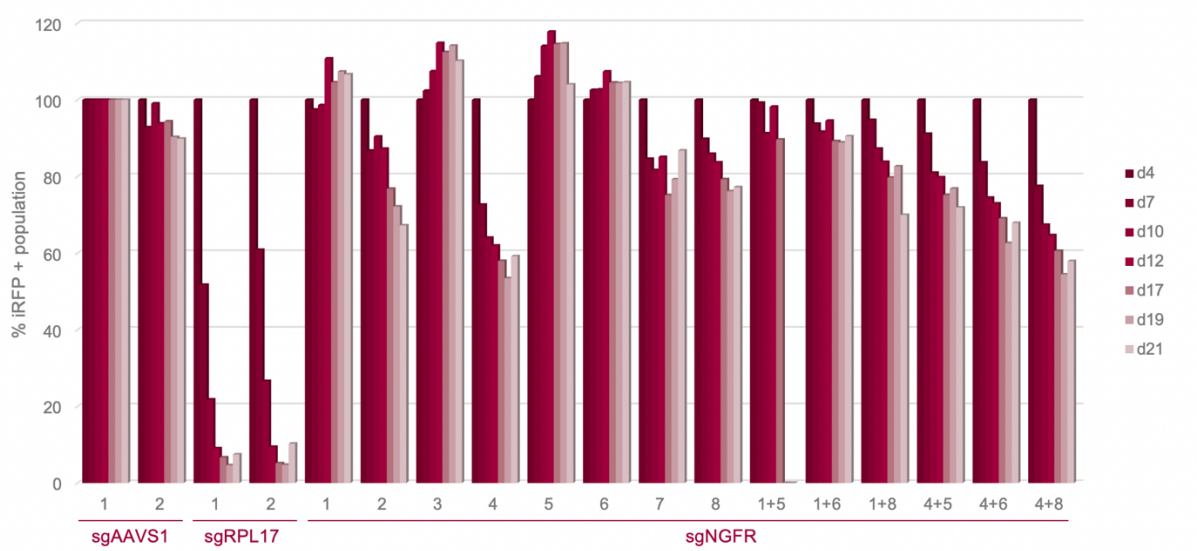


**Figure 10 - Growth competition assay 1: BMC1 Cas9-clone 10 + sgNGFR(1-8)**

Competition assay comparing the effectivity of different sgRNAs for NGFR as well as their combination in the cell line BMC1 Cas9-clone 10. Using sgAAVS1 as a negative control and sgRPL17 as a positive control. Percentages were normalized to sgAAVS1_1 on day 4.

Since we were not able to induce a full knock-out of NGFR in previous experiments, we decided to run a competition assay to compare the effectiveness of our different sgRNAs. Therefore, we induced knockouts using the CRISPR Cas9 system in the BMC1 clone 10 cell line, using different sgRNAs targeting NGFR at different positions.

In addition, we also tested the effect of combinations of sgRNAs. For that, we used one sgRNA targeting the N-terminus and one targeting the ICD fragment of NGFR. Since we discovered the presence of an in-frame ATG codon at position 236 that is surrounded by a Kozak sequence, we were hoping to achieve a full knock-out by directly targeting the ICD fragment.

We observed a significant drop in cell count, when using the positive control sgRPL17, demonstrating the reliability of the system. sgRPL17 leads to the mutational inactivation of the gene coding for the ribosomal protein L17, which is essential for cell survival, hence the drop in cell count. AAVS1 codes for the Adeno-Associated Virus Integration Site 1. Its knock-out has no impact on cell survival, hence the use as a negative control.

The use of sgNGFR_2 and sgNGFR_4 led to a distinct drop in cellular fitness over time. Similar effects were observed when sgNGFR_4 was combined with other sgRNAs. The use of sgNGFR_1, 3, 5, 6, 7 and 8 as well as the combination of sgNGFR_1 with other sgRNAs did not have an impact on cell count over time.

### 5.2. Comparison of BMC1 Cas9-clone 8 and clone 10: Western blot

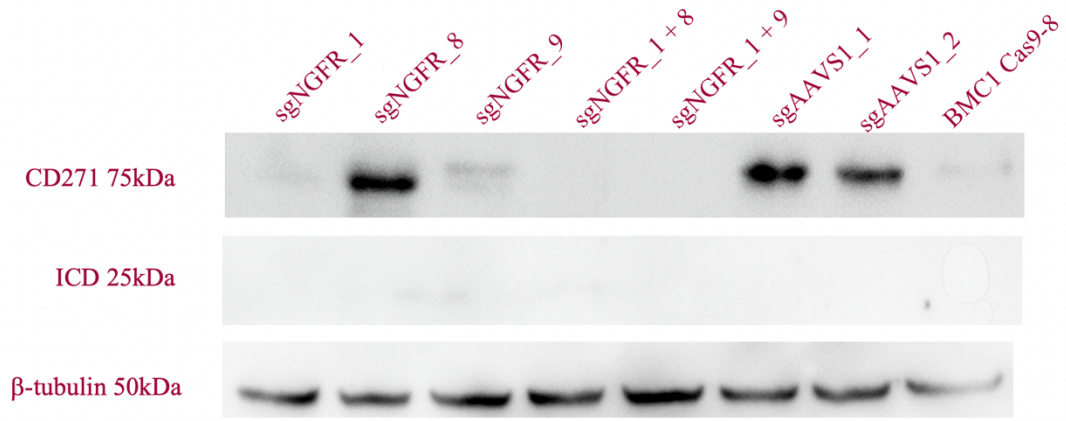


**Figure 11 - Western blot 1: BMC1 Cas 9- clone 8 + sgNGFR_1, 8 and 9 using an antibody against NGFR**

Western blot showing the levels of CD271 (NGFR) in BMC1-Cas9-clone 8 cells following CRISPR/Cas9 mediated knockout of CD271, using a polyclonal antibody against CD271 as well as a monoclonal antibody against β-tubulin. β-tubulin was used as a loading control.

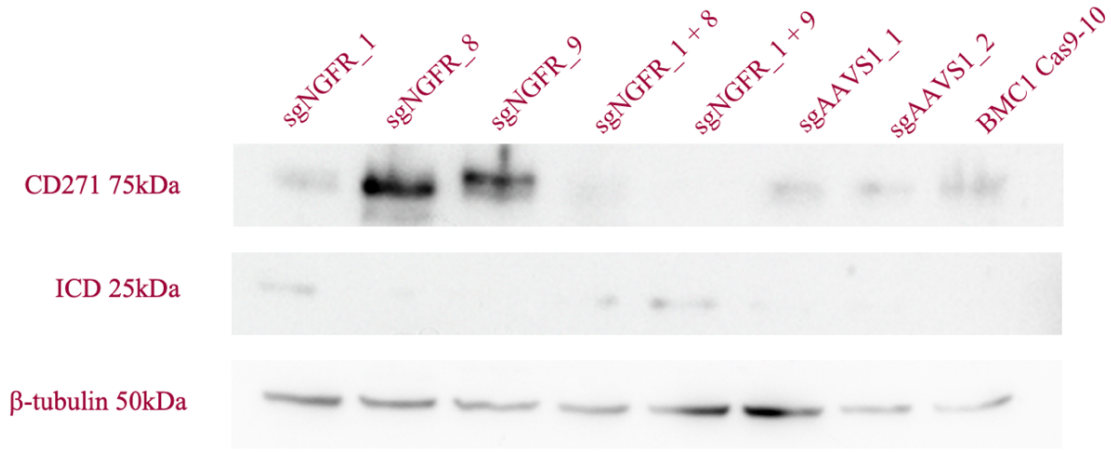


**Figure 12 - Western blot 2: BMC1 Cas 9- clone 10 + sgNGFR_1, 8 and 9 using an antibody targeting NGFR**

Western blot showing the levels of CD271 in BMC1-Cas9-clone 10 cells following a CRISPR/Cas9 mediated knockout of CD271 using a polyclonal antibody targeting CD271 as well as a monoclonal antibody targeting β-tubulin. β-tubulin was used as a loading control.

In previous experiments, we observed differences in NGFR expression when comparing BMC1 Cas9-clones 8 and clone 10. The clones were established from populations of cells which were sorted using the Fluorescent Activated Cell Sorter. Investigating the differences of NGFR expression in our clones is an important step to be able to carefully plan our future experiments. To investigate the difference between these two clones, we decided to induce knockouts of NGFR using the same sgRNAs as well as the combination of sgRNAs in the two different clones.

We decided to use one sgRNA targeting the N-terminus (sgNGFR_1) as well as two sgRNAs targeting the ICD fragment (sgNGFR_8 and 9) and the combination of both, in order to achieve a full knock-out of NGFR.

Western blot 1 shows the protein expression of NGFR in the BMC1 Cas9 clone 8. Strong expression of NGFR was found in BMC1 cells expressing the negative control sgAAVS_1. BMC1 Cas9-8 shows a lower NGFR expression. There is no band, neither at 75kDa nor at 25 kDa when the combination of sgNGFR_1 and sgNGFR_8/9 was used, which means that a full knock-out of NGFR was achieved using the combination of these sgRNAs.
In cells expressing sgNGFR_1, sgNGFR_8 and sgNGFR_9 we found a band at 75kDa representing NGFR. However, in the case of sgNGFR_1 the band is barely visible, which indicates that NGFR was not knocked out using these sgRNAs. The ICD fragment was never visible on this western blot.

Western blot 2 shows the protein expression of NGFR and the presumed ICD fragment in the BMC1 Cas9 clone 10. In cells expressing sgNGFR_1 we found a band at 75 kDa, as well as another one at 25 kDa. sgNGFR_8 and sgNGFR_9 show bands at 75 kDa but not at 25kDa. The combination of sgNGFR_1 and sgNGFR_8/9 abolished the expression of full length NGFR but allowed the expression of the 25kDa fragment. NGFR was expressed at equal levels in cells expressing sgAAVS_1 and in the BMC1 Cas9-10 line.
According to this western blot, a full knock-out of NGFR in BMC1 Cas9 clone 10 was never achieved using these sgRNAs.

### 5.3. Comparison of BMC1 Cas9-clone 8 and clone 10: Growth competition assay

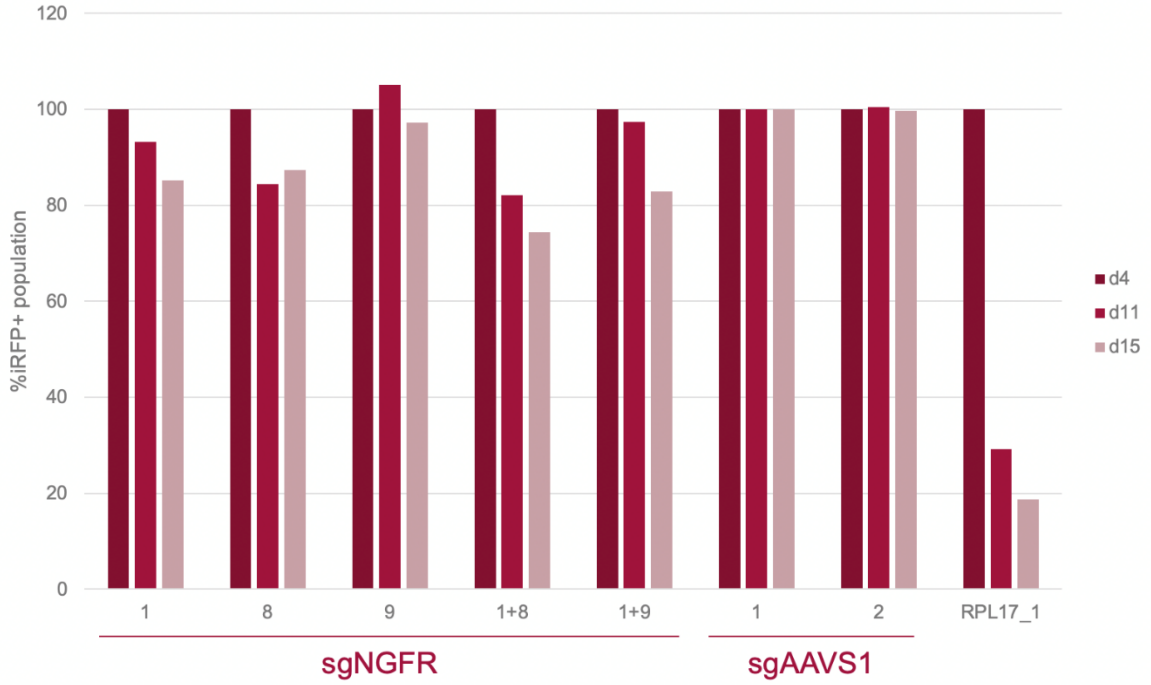


**Figure 13 - Growth competition assay 2: BMC1 Cas 9- clone 8 + sgNGFR_1, 8 and 9**

Competition assay comparing the effectivity of sg NGFR_1, 8, and 9 as well as their combination in the cell line BMC1 Cas9-clone 8. Using sgAAVS1 as a negative control and sgRPL17 as a positive control. Percentages were normalized to sgAAVS1_1 on day 4.

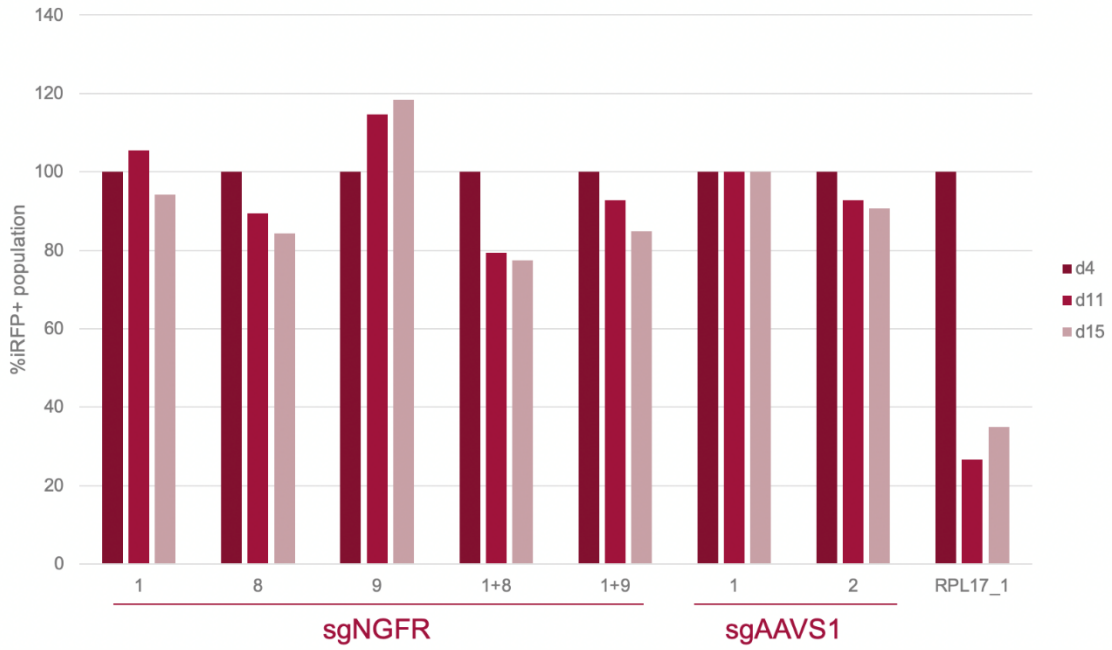


**Figure 14 - Growth competition assay 3: BMC1 Cas 9- clone 10 + sgNGFR_1, 8 and 9**

Competition assay comparing the effectivity of sg NGFR_1, 8 and 9 as well as their combination in the cell line BMC1 Cas9-clone 10. Using sgAAVS1 as a negative control and sgRPL17 as a positive control. Percentages were normalized to sgAAVS1_1 on day 4.

To investigate possible differences in NGFR expression between BMC1 Cas9-clone 8 and 10, we aimed to directly compare their response to CRISPR/Cas9-mediated NGFR inactivation. Since we also know from our western blot results which sgRNAs led to successful NGFR knock-out, we can also assess the effect of the NGFR knock-out or the ICD fragment on cell proliferation.

In growth competition assay 2, we observed a significant drop in cell counts when using our positive control sgRPL17, which again shows the reliability of the system. We also found a slight drop using sgNGFR_1 and sgNGFR_8 as well as in the combination of sgNGFR_1 with sgNGFR_8 and sgNGFR_9.

In growth competition assay 3, we can appreciate a drop in cell count, when using our positive control sgRPL17, even if there was a slight increase at day 15. We found a slight drop using sgNGFR_8. sgNGFR_9 did not have a negative effect on cell count but appeared to have a

positive effect on cell proliferation. However, the combination of sgNGFR_1 with sgNGFR_8 and sgNGFR_9 led to a slight drop in cell count.

### 5.4. NGFR protein levels upon MG132 treatment


**Figure 15 - Western blot 3: A375 + proteasome inhibitor MG132 (lower concentrations) using an antibody targeting NGFR**

Western blot membrane of A375 treated with MG132 for 8h, 16h and 24h using 0,25µM, 0,5µM and 1µM. Using a polyclonal antibody targeting NGFR, as well as a monoclonal antibody targeting β-tubulin.

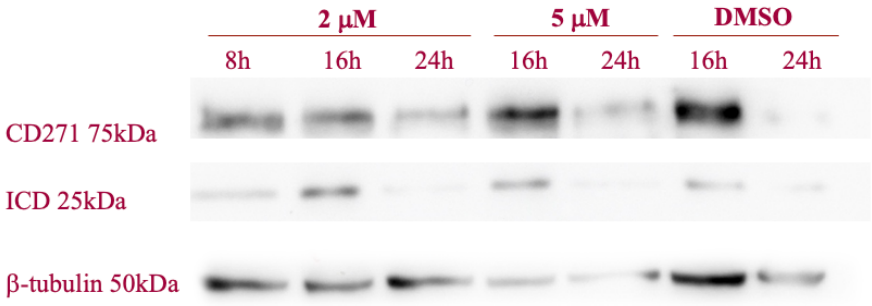


**Figure 16 - Western blot 4: A375 + proteasome inhibitor MG132 (higher concentrations) using an antibody targeting NGFR**

Western blot membrane of A375 treated with MG132 for 8h, 16h and 24h using 2µM, 5µM and DMSO. Using a polyclonal antibody targeting NGFR as well as a monoclonal antibody targeting β-tubulin.

According to a study by Saltari et al. in 2021, NGFR undergoes two proteolytic cleavage events, leading to the release of the CTF as well as the ICD. They hypothesized that the reduction of NGFR after 72 hours of treatment with a short peptide derived from beta-amyloid was due to the cleavage of NGFR, followed by the proteasomal degradation of its cleavage products.
They also showed that by treating cells overexpressing NGFR with the short peptide derived from beta-amyloid as well as the proteasome inhibitor MG132, they were able to detect the CTF as well as the ICD fragment in a western blot.
Thus, we wanted to prevent ICD degradation by using the proteasome inhibitor MG132 to have a closer look at the ICD fragment by Western Blotting.

In these western blots, we can appreciate a stable expression of the 25 kDa band. The 75 kDa band slightly increased with time, especially when comparing different time points within one concentration. At 2 μM, when comparing the 8h and 16h time points, we observed an increase in the intensity of the 25 kDa band. There was a decrease in the 75kDa and the 25kDa bands at 24h. This decrease was also observed at 5μM and with DMSO.

We are missing data for the 8h time point of two conditions (5 μM and DMSO) since we were not able to collect enough protein from samples from these conditions.

# 6. Discussion

As stated in the introduction, NGFR expression has been linked to aggressive disease progression, including a higher metastatic rate in melanoma (Redmer et al., 2014). It is also believed to work as a molecular switch promoting tumor progression (Filipp et al., 2019). As such, NGFR seems to be a promising driver of basic cellular properties in melanoma, such as migration, tumorigenicity, metastasis and plasticity. Additionally, as stated earlier, NGFR seems to play a role in the development of acquired resistances.

## 6.1. NGFR knock-out

To gain insight into the signaling mechanisms of NGFR, we wanted to achieve a full knockout of the latter in order to study its effects. Truzzi et al. were able to establish a link between NGFR and migration (Truzzi et al., 2008) and a study by Restivo et al. from 2017 implied that high levels of NGFR correlate with invasiveness (Restivo et al., 2017). These studies as well as our previous results from RNA-induced NGFR knockdown led us to the conclusion that NGFR knockout would lead to a proliferative disadvantage.

Keeping that in mind, it seems that in previous experiments, we were not successful in achieving a complete knock-out of NGFR using the CRISPR Cas9 system. In fact, we were not able to observe the expected drop in cell count associated with a proliferative disadvantage upon NGFR inactivation (Figure 5). Additionally, we observed a band appearing in our western blot at 25 kDa (Figure 6). These results led us to the discovery of a second in-frame translation initiation site surrounded by a Kozak sequence at position 236 and the question if the resulting ICD fragment could be responsible for counterbalancing the negative effect of the NGFR knock-out in our cell lines.

In order to gain more insight into this hypothesis, we decided to use different sgRNAs targeting NGFR to test their effectiveness as well as the combination of different sgRNAs targeting NGFR to investigate if this would lead to the expected phenotypic change.

Most of our sgRNAs did not lead to the phenotypic changes in cell growth that would be expected upon full NGFR knock-out, based on the results of the NGFR knock-down performed beforehand. While we observed a slight depletion of cell numbers, the expected changes from a full NGFR knock-out should be way more drastic, considering the effects of the NGFR knock-down.
However, sgNGFR_4 as well as its combination with other sgRNAs appeared to lead to a significant cell depletion, and the drop in cell counts correlated with the previous results of the NGFR knock-down. sgNGFR_2 also seemed to have an effect on cell survival.

It is important to note that the combination of sgNGFR_4 with other sgRNAs targeting the ICD fragment did not lead to a more prominent drop in cell count. In fact, the single use of sgNGFR_4 even seemed to be more effective. What needs to be considered here is that we cannot be sure that both sgRNAs have been integrated into the same cell in our co-infection experiments. In fact, since the expression of both sgRNAs is coupled to the same marker (iRFP670), we cannot differentiate between single- or double-infected cells. In order to make sure both sgRNAs are successfully integrated into the same cell, we would need to repeat this experiment using two different markers for the different sgRNAs.

It would have been interesting to have a western blot, of samples that represent cells used in competition assay #1 to see if we did indeed achieve a full knock-out of NGFR when using sgNGFR_2 and 4, as well as the combination of sgNGFR_4 with other sgRNAs. However, we did not perform a western blot in this experiment, since this experiment featured very inhomogeneous infection rates ranging from 15% to 75%, which makes the results not trustworthy.

According to this competition assay, the use of sgNGFR_4 to induce NGFR knockouts should definitely be considered for further experiments. Another interesting experiment would be to compare the single use of sgNGFR_4 to the combination of sgNGFR_4 with other sgRNAs targeting the ICD fragment. It would be interesting to have a direct comparison of phenotypic changes and protein expression. However, we would need to come up with another tagging system, using different markers when integrating two different sgRNAs in one cell line.

Sadly, we did not gain more information about the effect of the ICD fragment on cell proliferation. In fact, we would have needed a western blot investigating the presence of the ICD fragment to be able to correlate a certain phenotype with it. We do not know if the ICD is able to rescue the negative effect on cell survival of the NGFR knock-out or if the missing effect is simply due to the use of non-effective sgRNAs.

### 6.2. Comparison of BMC1 Cas9-clone 8 and 10

During previous experiments, we observed differences in NGFR expression when comparing BMC1 Cas9 clone 8 and clone 10. To further investigate the differences between these two clones, we decided to knockout NGFR using sgNGFR_1, 8 and 9 as well as combinations of sgNGFR_1 and sgNGFR8/9 in both clones. This information is important to properly plan future experiments.

According to our Western blots, the combinations of sgNGFR_1 and sg_NGFR8/9 in BMC1 Cas9 clone 8 led to a complete loss of NGFR expression. We also observed a slight depletion of cell numbers in the corresponding competition assay (Figure 13).
Even though we cannot be sure that both sgRNAs have been properly incorporated since their expression is coupled to the same marker (iRFP670), this western blot (Figure 11) might indicate that the combination of sgRNAs was successful since NGFR expression was lost when the combination of sgNGFR1 and sgNGFR8/9 was used. However, when using sgNGFR_1, NGFR expression was barely visible. This sgRNA caused a comparable drop in cell counts when compared to the combined use of sgNGFR_1 with sgNGFR_8/9.

We also noted a significant difference in NGFR expression between the negative control and the BMC1 Cas9 clone 8. We would presume that both cell lines should express the same levels of NGFR. The observed differences could be due to loading inconsistencies in the Western blot experiments. Another explanation could be that the stress associated with the virus infection to incorporate sgAAVS1 leads to increased NGFR expression. As discussed in the introduction, NGFR expression can be stress-induced.

When comparing BMC1 Cas9 clone 10 to clone 8, we are confronted with similar results in the competition assay. Yet, there seems to be a difference in NGFR and ICD expression between both clones. Interestingly, however, the western blot shows that we were not successful in achieving a full knock-out of NGFR in this experiment, as the full length NGFR and ICD fragments remained visible.

We also observed that sgNGFR_1 was less effective in BMC1 Cas9 clone 10. In the western blot, we were still able to detect bands at 75 kDa and 25kDa, proving the presence of the NGFR and the ICD fragment. Even the combination of sgNGFR_1 and sgNGFR_8/9 did not lead to a complete knock-out. Additionally, the BMC1 Cas 9 clone 10 seems to express higher levels of the ICD fragment when compared to the BMC1 Cas9 clone 8. Further experiments would be needed to confirm this.
These results led us to the assumption that there must be a difference between BMC1 Cas9 clone 8 and clone 10, which has to be taken into consideration for further experiments.

### 6.3. Proteasomal degradation of the ICD fragment

As stated before, a study by Saltari et al. in 2021 proved that the ICD fragment undergoes proteasomal degradation. They were able to inhibit this by adding the proteasome inhibitor MG132. To have a closer look at the ICD fragment by Western blotting we decided to use the same proteasome inhibitor.
Indeed, proteasome inhibition led to increased expression of the ICD fragment, which cannot reliably be detected in Western blots. However, we were expecting the expression to increase with treatment time, which was not fully reflected by our results.
In fact, we only found a significant increase in the expression of the NGFR 25kDa fragment at 2 μM when comparing the 8h time point to the 16h timepoint. However, we also noticed a decrease in the expression at the 24h timepoint. This could be linked to the fact the cells start to die after a certain time, as the proteasome inhibitor interferes with the normal cell machinery. We would also expect the expression to increase with increasing inhibitor concentrations, but this is not reflected by our results. In fact, expression of the 25 kDa fragment seemed to be lower at 2 μM than at 1 μM, during the same treatment periods. This could be linked to inhomogeneous loading concentrations.

Another issue is that we observed a decrease in NGFR expression upon DMSO treatment. This could be linked to DMSO-inducing cell stress or inhomogeneous loading.

As a conclusion, we were indeed able to stop ICD degradation by using the proteasome inhibitor MG132, allowing us to have a closer look at the ICD fragment. However, due to the inconclusive results, this experiment should be repeated. It would be interesting to investigate the effects of MG132 over a shorter period of time, using different time points. It also has to be noted that proper controls should be used for every western blot.

## 7. Conclusion

The results of previous experiments prompted us to take a closer look at NGFR and its ICD fragment to understand why we were unable to replicate the same phenotypical changes when comparing NGFR knock-out and knock-down.

We were not able to solve the question if the ICD fragment is able to rescue the negative effects of the NGFR knock-out. It would be interesting to know if the ICD fragment is able to rescue the knock-out. Our Western Blot results from the experiments using combinations of sgRNAs indicate that this could be the case, However, we cannot be sure that both sgRNAs have been incorporated into the cell since both are marked with the iRFP670 fluorescence reporter. We would need to repeat the experiments using two different markers for the different sgRNAs in order to properly analyze our results.

The experiments should be repeated with more care, making sure to reach homogenous infection rates, putting more time into planning and using proper controls, in order to achieve trustworthy and reproducible results.

More experiments would be needed to reach a final conclusion. However, we can say that the ICD fragment appears to play an important role in rescuing the negative effects of an NGFR knock-out. If true, this could make the NGFR ICD fragment an important therapeutic target.

## 8. Bibliography


Akbani, R., Akdemir, K. C., Aksoy, B. A., Albert, M., Ally, A., Amin, S. B., Arachchi, H., Arora, A., Auman, J. T., Ayala, B., Baboud, J., Balasundaram, M., Balu, S., Barnabas, N., Bartlett, J., Bartlett, P., Bastian, B. C., Baylin, S. B., Behera, M., … Zou, L. (2015). Genomic Classification of Cutaneous Melanoma. *Cell*, *161*(7), 1681–1696. https://doi.org/10.1016/j.cell.2015.05.044

Balch, C. M., Gershenwald, J. E., Soong, S. J., Thompson, J. F., Atkins, M. B., Byrd, D. R., Buzaid, A. C., Cochran, A. J., Coit, D. G., Ding, S., Eggermont, A. M., Flaherty, K. T., Gimotty, P. A., Kirkwood, J. M., McMasters, K. M., Mihm, M. C., Morton, D. L., Ross, M. I., Sober, A. J., & Sondak, V. K. (2009). Final version of 2009 AJCC melanoma staging and classification. *Journal of Clinical Oncology*, *27*(36), 6199–6206. https://doi.org/10.1200/JCO.2009.23.4799

Bao, X., Shi, J., Xie, F., Liu, Z., Yu, J., Chen, W., Zhang, Z., & Xu, Q. (2018). Proteolytic release of the p75 NTR intracellular domain by adam10 promotes metastasis and resistance to anoikis. *Cancer Research*, *78*(9), 2262–2276. https://doi.org/10.1158/0008-5472.CAN-17-2789

Barman, A., Deb, B., & Chakraborty, S. (2020). A glance at genome editing with CRISPR–Cas9 technology. In *Current Genetics* (Vol. 66, Issue 3, pp. 447–462). Springer. https://doi.org/10.1007/s00294-019-01040-3

Bhatia, S., Tykodi, S. S., & Thompson, J. A. (2009). *Treatment of Metastatic Melanoma: An Overview Prognostic Factors for Metastatic Melanoma*.

Boiko, A. D., Razorenova, O. v., van de Rijn, M., Swetter, S. M., Johnson, D. L., Ly, D. P., Butler, P. D., Yang, G. P., Joshua, B., Kaplan, M. J., Longaker, M. T., & Weissman, I. L. (2010). Human melanoma-initiating cells express neural crest nerve growth factor receptor CD271. *Nature*, *466*(7302), 133–137. https://doi.org/10.1038/nature09161

Chen, Y., Zeng, J., Wang, X., Yao, G., Wang, W., Qi, W., & Kong, K. (2009). Multiple Roles of the p75 Neurotrophin Receptor in the Nervous System. In *The Journal of International Medical Research* (Vol. 37).

Curtin, J. A., Fridlyand, J., Kageshita, T., Patel, H. N., Busam, K. J., Kutzner, H., Cho, K.-H., Aiba, S., Bröcker, E.-B., Leboit, P. E., Pinkel, D., & Bastian, B. C. (2005). Distinct Sets of Genetic Alterations in Melanoma. In *n engl j med* (Vol. 20). www.nejm.org

Daneman, R., & Prat, A. (2015). The blood–brain barrier. *Cold Spring Harbor Perspectives in Biology*, *7*(1). https://doi.org/10.1101/cshperspect.a020412

Dankort, D., Curley, D. P., Cartlidge, R. A., Nelson, B., Karnezis, A. N., Damsky, W. E., You, M. J., DePinho, R. A., McMahon, M., & Bosenberg, M. (2009). BrafV600E cooperates with Pten loss to induce metastatic melanoma. *Nature Genetics*, *41*(5), 544–552. https://doi.org/10.1038/ng.356

DeVita, V. T. Jr., Lawrence, T. S., & Rosenberg, S. A. (2011). *DeVita, Hellman, and Rosenberg's Cancer: Principles & Practices of Oncology* (9th Edition). Lippincott Williams & Wilkins, a Wolters Kluwer business.

Doudna, J. A., & Charpentier, E. (2014). *The new frontier of genome engineering with CRISPR-Cas9*. http://science.sciencemag.org/

Filipp, F. v., Li, C., & Boiko, A. D. (2019). CD271 is a molecular switch with divergent roles in melanoma and melanocyte development. *Scientific Reports*, *9*(1). https://doi.org/10.1038/s41598-019-42773-y

Flaherty, K. T., Robert, C., Hersey, P., Nathan, P., Garbe, C., Milhem, M., Demidov, L. v., Hassel, J. C., Rutkowski, P., Mohr, P., Dummer, R., Trefzer, U., Larkin, J. M. G., Utikal, J., Dreno, B., Nyakas, M., Middleton, M. R., Becker, J. C., Casey, M., … Schadendorf, D. (2012). Improved Survival with MEK Inhibition in BRAF-Mutated Melanoma. *New England Journal of Medicine*, *367*(2), 107–114. https://doi.org/10.1056/nejmoa1203421

Glitza, I. C., Heimberger, A. B., Sulman, E. P., & Davies, M. A. (2016). Prognostic Factors for Survival in Melanoma Patients with Brain Metastases. In *Brain Metastases from Primary Tumors: Epidemiology, Biology, and Therapy of Melanoma and Other Cancers* (Vol. 3, pp. 267–297). Elsevier Inc. https://doi.org/10.1016/B978-0-12-803508-5.00019-6

Gray-Schopfer, V., Wellbrock, C., & Marais, R. (2007). Melanoma biology and new targeted therapy. In *Nature* (Vol. 445, Issue 7130, pp. 851–857). Nature Publishing Group. https://doi.org/10.1038/nature05661

Guo, W., Wang, H., & Li, C. (2021). Signal pathways of melanoma and targeted therapy. In *Signal Transduction and Targeted Therapy* (Vol. 6, Issue 1). Springer Nature. https://doi.org/10.1038/s41392-021-00827-6

Guo, Y., Pan, W., Liu, S., Shen, Z., Xu, Y., & Hu, L. (2020). ERK/MAPK signalling pathway and tumorigenesis (Review). *Experimental and Therapeutic Medicine*. https://doi.org/10.3892/etm.2020.8454

Herrmann, J. L., Menter, D. G., Hamada, J.-I., Marchetti, D., Nakajima, M., & Nicolson, G. L. (1993). Mediation of NGF-stimulated Extracellular Matrix Invasion by the Human Melanoma Low-affinity p75 Neurotrophin Receptor: Melanoma p75 Functions Independently of trkA. In *Molecular Biology of the Cell* (Vol. 4).

Kienast, Y., von Baumgarten, L., Fuhrmann, M., Klinkert, W. E. F., Goldbrunner, R., Herms, J., & Winkler, F. (2010). Real-time imaging reveals the single steps of brain metastasis formation. *Nature Medicine*, *16*(1), 116–122. https://doi.org/10.1038/nm.2072

Kim, C. J., Reintgen, D. S., Balch, C. M., & Lee, H. (2002). *The New Melanoma Staging System From the Departments of Surgery (CJK, DSR) and Cutaneous Oncology Program (DSR), at the*.

Lehraiki, A., Cerezo, M., Rouaud, F., Abbe, P., Allegra, M., Kluza, J., Marchetti, P., Imbert, V., Cheli, Y., Bertolotto, C., Ballotti, R., & Rocchi, S. (2015). Increased CD271 expression by the NF-kB pathway promotes melanoma cell survival and drives acquired resistance to BRAF inhibitor vemurafenib. *Cell Discovery*, *1*. https://doi.org/10.1038/celldisc.2015.30

Lin, W. M., & Fisher, D. E. (2017). Signaling and Immune Regulation in Melanoma Development and Responses to Therapy. In *Annual Review of Pathology: Mechanisms of Disease* (Vol. 12, pp. 75–102). Annual Reviews Inc. https://doi.org/10.1146/annurev-pathol-052016-100208

Long, G. v., Fung, C., Menzies, A. M., Pupo, G. M., Carlino, M. S., Hyman, J., Shahheydari, H., Tembe, V., Thompson, J. F., Saw, R. P., Howle, J., Hayward, N. K., Johansson, P., Scolyer, R. A., Kefford, R. F., & Rizos, H. (2014). Increased MAPK reactivation in early resistance to dabrafenib/trametinib combination therapy of BRAF-mutant metastatic melanoma. *Nature Communications*, *5*. https://doi.org/10.1038/ncomms6694

McArthur, G. A., Chapman, P. B., Robert, C., Larkin, J., Haanen, J. B., Dummer, R., Ribas, A., Hogg, D., Hamid, O., Ascierto, P. A., Garbe, C., Testori, A., Maio, M., Lorigan, P., Lebbé, C., Jouary, T., Schadendorf, D., O'Day, S. J., Kirkwood, J. M., … Hauschild, A. (2014). Safety and efficacy of vemurafenib in BRAFV600E and BRAFV600K mutation-positive melanoma (BRIM-3): Extended follow-up of a phase 3, randomised, open-label study. *The Lancet Oncology*, *15*(3), 323–332. https://doi.org/10.1016/S1470-2045(14)70012-9

McCain, J. (2013). The MAPK (ERK) Pathway: Investigational Combinations for the Treatment Of BRAF-Mutated Metastatic Melanoma. *P & T : A Peer-Reviewed Journal for Formulary Management*, *38*(2), 96–108. https://pubmed.ncbi.nlm.nih.gov/23599677

Menon, D. R., Das, S., Krepler, C., Vultur, A., Rinner, B., Schauer, S., Kashofer, K., Wagner, K., Zhang, G., Bonyadi Rad, E., Haass, N. K., Soyer, H. P., Gabrielli, B., Somasundaram, R., Hoefler, G., Herlyn, M., & Schaider, H. (2015). A stress-induced early innate response causes multidrug tolerance in melanoma. *Oncogene*, *34*(34), 4448–4459. https://doi.org/10.1038/onc.2014.372

Menzies, A. M., Long, G. v., & Murali, R. (2012). Dabrafenib and its potential for the treatment of metastatic melanoma. In *Drug Design, Development and Therapy* (Vol. 6, pp. 391–405). https://doi.org/10.2147/DDDT.S38998

Ngo, M., Han, A., Lakatos, A., Sahoo, D., Hachey, S. J., Weiskopf, K., Beck, A. H., Weissman, I. L., & Boiko, A. D. (2016). Antibody Therapy Targeting CD47 and CD271 Effectively Suppresses Melanoma Metastasis in Patient-Derived Xenografts. *Cell Reports*, *16*(6), 1701–1716. https://doi.org/10.1016/j.celrep.2016.07.004

Randic, T., Kozar, I., Margue, C., Utikal, J., & Kreis, S. (2021). NRAS mutant melanoma: Towards better therapies. In *Cancer Treatment Reviews* (Vol. 99). W.B. Saunders Ltd. https://doi.org/10.1016/j.ctrv.2021.102238

Redmer, T. (2018). Deciphering mechanisms of brain metastasis in melanoma - the gist of the matter. In *Molecular Cancer* (Vol. 17, Issue 1). BioMed Central Ltd. https://doi.org/10.1186/s12943-018-0854-5

Redmer, T., Welte, Y., Behrens, D., Fichtner, I., Przybilla, D., Wruck, W., Yaspo, M. L., Lehrach, H., Schäfer, R., & Regenbrecht, C. R. A. (2014). The nerve growth factor receptor CD271 is crucial to maintain tumorigenicity and stem-like properties of melanoma cells. *PLoS ONE*, *9*(5). https://doi.org/10.1371/journal.pone.0092596

Restivo, G., Diener, J., Cheng, P. F., Kiowski, G., Bonalli, M., Biedermann, T., Reichmann, E., Levesque, M. P., Dummer, R., & Sommer, L. (2017). Low Neurotrophin receptor CD271 regulates phenotype switching in Melanoma. *Nature Communications*, *8*(1). https://doi.org/10.1038/s41467-017-01573-6

Robert, C., Karaszewska, B., Schachter, J., Rutkowski, P., Mackiewicz, A., Stroiakovski, D., Lichinitser, M., Dummer, R., Grange, F., Mortier, L., Chiarion-Sileni, V., Drucis, K., Krajsova, I., Hauschild, A., Lorigan, P., Wolter, P., Long, G. v., Flaherty, K., Nathan, P., … Schadendorf, D. (2015). Improved Overall Survival in Melanoma with Combined Dabrafenib and Trametinib. *New England Journal of Medicine*, *372*(1), 30–39. https://doi.org/10.1056/nejmoa1412690

Saltari, A., Dzung, A., Quadri, M., Tiso, N., Facchinello, N., Hernandez-Barranco, A., Garcia-Silva, S., Nogues, L., Stoffel, C. I., Cheng, P. F., Turko, P., Eichhoff, O. M., Truzzi, F., Marconi, A., Pincelli, C., Peinado, H., Dummer, R., & Levesque, M. P. (2021). Specific Activation of the CD271 Intracellular Domain in Combination with Chemotherapy or Targeted Therapy Inhibits Melanoma Progression. *Cancer Research*, *81*(23), 6044–6057. https://doi.org/10.1158/0008-5472.CAN-21-0117

Smith, M. P., Brunton, H., Rowling, E. J., Ferguson, J., Arozarena, I., Miskolczi, Z., Lee, J. L., Girotti, M. R., Marais, R., Levesque, M. P., Dummer, R., Frederick, D. T., Flaherty, K. T., Cooper, Z. A., Wargo, J. A., & Wellbrock, C. (2016). Inhibiting Drivers of Non-mutational Drug Tolerance Is a Salvage Strategy for Targeted Melanoma Therapy. *Cancer Cell*, *29*(3), 270–284. https://doi.org/10.1016/j.ccell.2016.02.003

Sun, L., Lutz, B. M., & Tao, Y.-X. (2016). *The CRISPR/Cas9 system for gene editing and its potential application in pain research*.

Truzzi, F., Marconi, A., Lotti, R., Dallaglio, K., French, L. E., Hempstead, B. L., & Pincelli, C. (2008). Neurotrophins and their receptors stimulate melanoma cell proliferation and migration. *Journal of Investigative Dermatology*, *128*(8), 2031–2040. https://doi.org/10.1038/jid.2008.21

Vidal, A., & Redmer, T. (2020). Decoding the role of CD271 in Melanoma. In *Cancers* (Vol. 12, Issue 9, pp. 1–19). MDPI AG. https://doi.org/10.3390/cancers12092460

## 9. Table of figures